IONOSPHERIC SIGNAL PROPAGATION SIMULATOR FOR EARTH OBSERVATION MISSIONS

Elena Fernández-Niño[1], Carlos Molina[1,2], and Adriano Camps[1,2]

[1]CommSensLab – UPC, Universitat Politècnica de Catalunya – BarcelonaTech
[2]Institute of Space Studies of Catalonia (IEEC) – CTE – UPC

ABSTRACT

Following the discovery of the ionosphere by Marconi in 1901, different disciplines have been influenced from the ionospheric effects on radio-waves, such as communications or Earth Observation missions. The ionosphere acts as an electrical layer that is continuously changing due mainly to solar activity. Therefore, it is not a trivial work to predict how radio signals would be affected. This study presents the implementation of a Matlab ray-tracer to predict radio-wave propagation through the ionosphere. This program is inspired on a Fortran code developed in the 70's, but it is extended to include the state-of-the-art models, such as the IRI (International Reference Ionosphere), the IGRF (International Geomagnetic Reference Field), and the NRLMSISE-00 (Naval Research Lab, atmospheric model). A statistical model of bubbles and depletions is also included for increased accuracy. The simulator provides several graphs and a text document, both summarizing the ray trajectories and main propagations effects. This tool is being developed as part of an ESA project devoted to the study of ionospheric effects in low frequency radars, namely radar sounders and Synthetic Aperture Radars, and GNSS systems.

Index Terms— Ionosphere, ray tracer, range-delay, phase-advance, refraction, absorption, dispersion, Faraday rotation

1. INTRODUCTION

The discovery of the ionosphere dates back to 1901 when Marconi was conducting his first trans-Atlantic communications between Wales and Newfoundland, although at that time he was not conscious of its existence. Nowadays, the ionosphere is typically categorized into 3 layers: D extending from 50 to 90 km, E extending from 90 to 130 km, and F. The F layer is divided into 2 sublayers: F_1 extending from 130 to 210 km and F_2 extending from 210 to above 2000 km. Even though, it is not considered a stratified layer, since it changes according to the rotation (day and night), and translation (seasons of the year) movements of the Earth. This is due to the fact that the composition of the ionosphere depends, to a large extent, on the solar activity and, to a lesser extent, on Earth's magnetic field, cosmic rays and other celestial bodies. Consequently, the electron density is constantly altered due to the variation of solar radiation.

When an electromagnetic wave passes through the ionosphere, different effects modify the initial properties of the ray. The identified effects are dispersion, refraction, absorption, range-delay, phase-advance, scintillation, signal fading and Faraday rotation [1]. However, not all of them affect signals in the same way. It depends on the characteristics of the signal (e.g., frequency, elevation, and azimuth angles), and on the electron density of the ionospheric zone crossed.

Therefore, all space sciences are in principle conditioned by the distortions produced in signals by the ionosphere, especially those operating at low frequencies.

Earth Observation missions such as ALOS-PALSAR, ROSE-L, NISAR, SAOCOM, or BIOMASS, are based in Synthetic Aperture Radar (SAR) technology. All of them operate at L-band, except BIOMASS which operates at P-band. This technology bases its processing on the signal phase. The spatial fluctuations of the ionospheric Total Electron Content (TEC) can distort the focusing of the received echoes due to the phase-advance, range-delay, dispersion, Faraday rotation, and ionospheric scintillation, resulting in blurred target images.

Furthermore, the Global Navigation Satellite Systems-Reflectometry (GNSS-R) missions are also affected by the ionosphere. This remote sensing technique takes advantage of opportunistic signals sent from GNSS satellites. Its method is based on calculating the ratio of the intensities and for the delay difference between the direct signals, and those reflected from the Earth. Consequently, this technique must face an even more complex problem than the previous one. The GNSS signals cross all the ionospheric layers along the 3 different paths that define the GNSS-R shape, instead of the 2 identical paths as in SAR. Therefore, the signals are influenced by TEC fluctuations and ionospheric scintillation effects.

Additionally, the NASA and Qatar OASIS mission [2] requires VHF radar sounder technology to find traces of underground water in arid areas. Similar technologies have been proposed to study the ice stratification. The radar operates at 45 MHz. In this way, it can penetrate up to 100 meters depth. At these frequencies, the ionosphere can still be considered an almost transparent layer. Nevertheless,

 DOI: 10.1109/IGARSS46834.2022.9883781

targeting larger depths future missions will have to use lower frequencies to achieve this goal, and ionospheric effects will start becoming noticeable. In the limit the ionosphere will behave as a reflective layer deflecting the signals. In the radar sounder case, the effects on the signals transmitted are diffraction, refraction, absorption, Faraday rotation, and scintillation, among others.

Finally, satellite communication missions may also be affected by this conductive layer due to their low working frequency. For example, the MUOS constellation [3] operates at VHF-UHF bands. At this frequency range, the most important is the effect scintillation.

This project is part of an ionospheric simulator project, called SIMIONO, being developed for ESA, in collaboration with ONERA (France), and RDA (Switzerland). So, the UPC NanoSat-Lab team is responsible for the development of the ionospheric ray-tracing and scintillation modules. The ray-tracer is presenter here.

The simulator is based on a Fortran tool developed in 1975 by R. M. Jones and J. J. Stephenson [4]. The first thing was the conversion from Fortran to Matlab. Then, the following updated models have been integrated: the International Reference Ionosphere (IRI) [5] providing the electron density profile; the International Geomagnetic Reference Field (IGRF) [6] for the Earth's magnetic field model; the NRLMSISE-00 [7] providing the atmospheric composition model; and the bubbles and depletions model [8] developed in the framework of SCIONAV. In this way, the simulator models the effects produced by the ionosphere on radio waves, even though many of them can be ignored at high frequencies, since it can be considered a transparent layer.

2. SIMULATOR MODELS

Over these nearly five decades since the original Fortran code [4], new models have been developed to better predict the behavior of the electron density, the Earth's magnetic field, and the atmospheric composition. They are included in our code.

The next block diagram summarizes simulator performance. It is divided into 2 sections: the user interface, or "UI", and the propagator module. First, the "UI" module inputs the variables stated by the user, and calls the propagator system, or "MAIN_RT". It also provides the simulation results to the user at the end of the simulation. The next section starts with the "MAIN_RT" block, which sets the initial ray condition and calls tracing functions. The "TRACE" couple evaluates stop condition according to the current ray position. The ray propagation is computed by integrating and evaluating Hamiltonian differential equations in "RKAM" and "HAMILTON", respectively. The refractive index and related concepts are computed in the "RINDEX" block. This is done considering if collisions module is activated or not. This last block also depends on the data computed from all models explained in section 2. The electron density from IRI model is evaluated in "ELECT_DENS"; the "PERT" block call for bubbles and depletion model; the IGRF is called from "MAG_FIELD"; and the NRLMSISE-00 is used in "COL_FREQ". These methods are explained in the next sections.

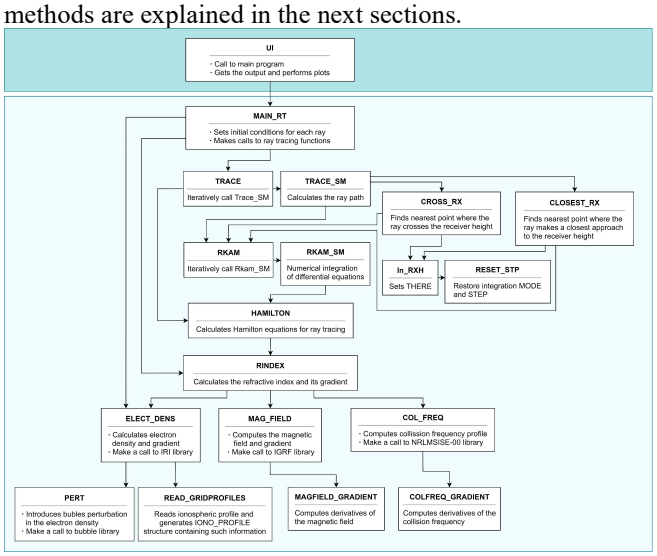

Fig. 1. Block diagram of the ray tracer

2.1. Ionospheric model: IRI

The International Reference Ionosphere, also referred to as IRI, is an ionospheric model developed in 1960 by COSPASAR and URSI [5]. This model is based on measurements from different ionosondes and satellites, among others.

IRI provides information on the electron density or ion species as a function of height. Fig. 2 illustrates the ionospheric electron density profile for March 21st, 2014, at 6:50 UTC. Note that the solar cycle reached its peak in March 2014 and, consequently, the ionospheric activity. Specifically, an average of 128.7 sunspots per month were recorded at that time [9].

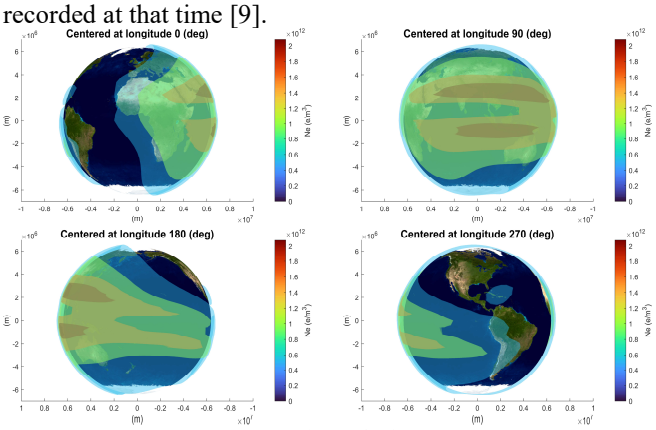

Fig. 2. 3D ionospheric map

2.2. Earth's magnetic field model: IGRF

The Earth's magnetic field also influences the ionosphere. It has been modeled using the International Geomagnetic Reference Field, or IGRF [6]. This model is updated every 5

years by the International Association of Geomagnetism and Aeronomy (IAGA).

2.3. Atmospheric model: NRLMSISE-00

The electromagnetic waves attenuation is governed by the collisions between particles. Nevertheless, since the frequency collision depends on their density and the temperature, an atmospheric model is necessary. The NRLMSISE-00 atmospheric model is used to obtain the altitude profile of atomic and molecular densities, and temperature. Figure 3 illustrates how plasma electron density (a), atmospheric gas density and temperature (b) are distributed at different altitudes.

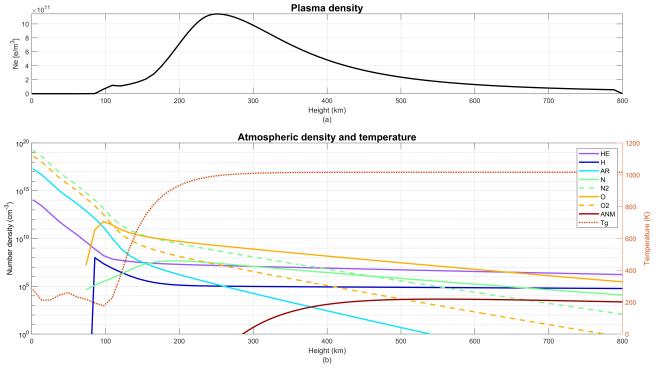

Fig. 3. (a) Plasma density and (b) atmospheric density and temperature

3. SAMPLE RESULTS

The simulator integrates the data extracted from previous models into the ray propagation program, which produces along the ray path different effects of the ionosphere.

3.1. Dispersion and refraction

First, the gyrofrequency is computed from the magnetic field coefficients provided by IGRF model, and the electron density and the plasma frequency are taken from IRI.

At low frequencies, the ionosphere can refract the electromagnetic waves, which may eventually bend back appearing as being "reflected" at an upper layer. So, following scenario (Fig. 4) simulates the behavior of 8 frequency shifted signals emitted with an elevation angle of -35° wrt. to the line of sight. The satellite is at 800 km height, 41.39° latitude, and 2.15° longitude. While the signals stop at 1000 km of altitude.

It can be seen that signal paths bend around F layer (300 km height) due to the higher electron density of the ionosphere (see Fig. 5). While higher frequency signals pass through the ionosphere and reaches ground, the lower ones are reflected back to outer space. Additionally, the 13 MHz signal (green color) is the first one that completely crosses the ionosphere. So, it is the one that has the most curved path. This geometry is very interesting for long distance communication services.

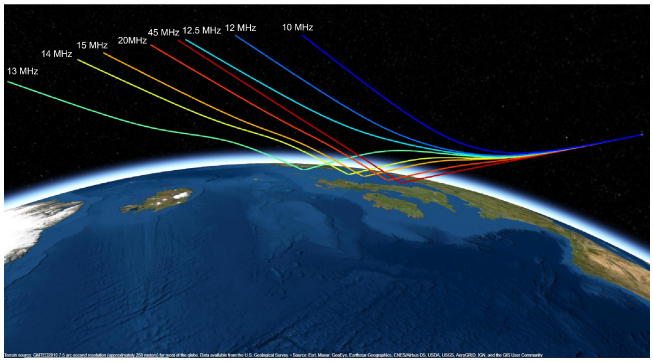

Fig. 4. Dispersion and refraction effects

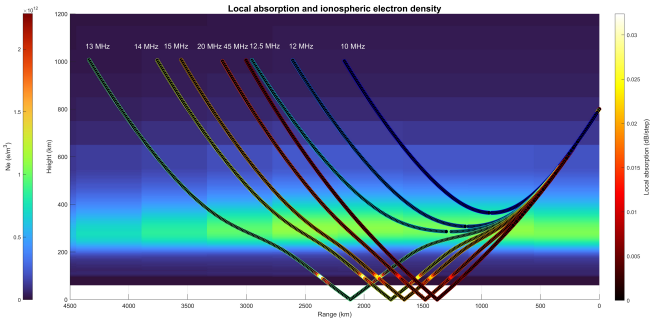

Fig. 5. Local absorption as a function of altitude

3.2. Absorption, phase-advance and range-delay

The atmosphere is composed by atoms and molecules (see Fig. 3b). The ionosphere is composed by ions and free electrons, originated from the collisions between the incoming particles and atmospheric gases. Collisions cause the absorption, which is more important at the D and E layers because of the higher gas's density as compared to the F layer. In Fig. 3a, the high gas density leads to the first peak, as the second one is due to the high plasma density in F layer, and it is responsible for the ray's bending as seen section 3.1. The collision frequency is computed as stated in [10], where atmospheric parameters (temperature and density) are provided by NRLMSISE-00 model.

While the absorption is modeled by the imaginary part of the refractive index, the real part leads to the propagation of the ray, specifically, the propagation speed and the bending angle. When the refractive index is equal to 1, the signal propagates following a linear trajectory. However, when the signal is in the ionosphere, the refractive index is less than 1, the speed decreases resulting in a phase-advance, and the ray bends causing a range-delay.

The simulator computes the local and cumulative absorptions along the path. Fig. 5 shows the local absorption of previous 8 signals, and a vertical ionospheric cut at 2.15° longitude to relate the ray curvature to the electron content at F layer. Table 1 indicates the total absorption of each ray.

Table 1. Cumulative absorption

Freq. [MHz]	10	12.5	12	13	14	15	20	45
Cum. abs. [dB]	0.001	0.002	0.004	0.357	0.284	0.249	0.126	0.026

It can be deduced from table 1 that at lower frequencies the total absorption increases, except for the first 3 low frequency signals since they do not reach the E layer.

3.3. Faraday rotation

An interesting effect produced in the propagation of electromagnetic waves in an ionized media in the presence of a magnetic field is the rotation of the polarization plane or "Faraday rotation". When the ray is propagating it splits into 2 rays (birefringence effect). The one that travels in the perpendicular direction with respect to the magnetic field is called the ordinary ray; while the one that propagates through the normal direction is the extraordinary ray. When this occurs, the 2 rays traverse different paths through the ionosphere, and have different refractive indices. Therefore, they may have different absorptions and delays, which is ultimately responsible for the rotation of the polarization plane. The next scenario has been set to appreciate this effect. It performs a HF radar sounder with the same initial coordinates than the previous one. The frequency is set to 8 MHz and the down-looking angle is -90°.

Fig. 6 illustrates in the propagation of the ordinary (blue) and extraordinary (red) rays, the local absorption along the path, and the ionospheric electron density. It can be seen how the ray bends, and splits into 2 rays. At the output, both rays are parallel and the two plane waves "add together" with a different relative phase than when they split around the F layer, leading to the Faraday rotation. Additionally, the ordinary and extraordinary cumulative absorptions are 0.147 dB and 0.243 dB, respectively.

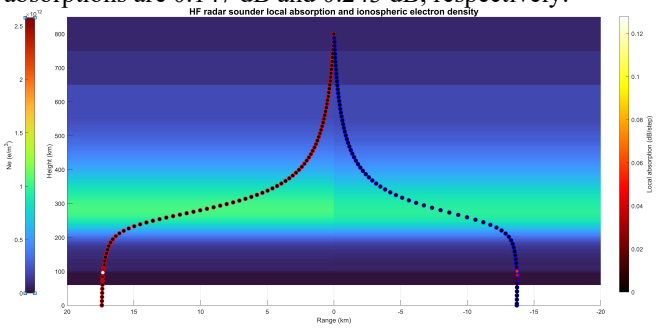

Fig. 6. Local absorption of ordinary and extraordinary rays

4. CONCLUSIONS

The ionosphere influences all missions, but especially those operating at low frequencies, from HF to L-band. The main objective of this simulator is the propagation of electromagnetic signals through the ionosphere regardless of the technology onboard the satellite. Therefore, it can be used for predicting ionospheric effects and preventing signal distortions in SAR, GNSS-R or Radar sounders missions.

The first thing was to convert the Fortran 77 to Matlab language in order make the code more intelligible. However, the conversion did not work properly, and it was necessary to review and address some issues. In addition, the design and implementation of several state machines has been essential for the program flow control. Likewise, this conversion also made it easier to debug the code.

The incorporation of the complex IRI, IGRF, and NRLMSISE-00 models makes the simulator a powerful propagation tool never developed before. Consequently, many of the initial functions have been reprogrammed to deal with the data obtained from these models.

Despite current functionalities, there are different lines of work in progress to improve the simulator. Specifically, a 3-dimensional (range, azimuth, and height) bubbles generator is being developed to perform disturbances and improve the accuracy of the signal trajectory. It is based on the 2-dimensional bubble model generated by RDA, gAGE/UPC and Ebre Observatory in the SCIONAV project for ESA. The next version will also have scintillation effects.

Furthermore, the use of this simulator can be extended to other applications thanks to its versatility in the introduction of new profiles. For example, it can also be used to find proper mitigation techniques during the spacecraft reentry stage to avoid blackout effect.

5. REFERENCES

[1] ITU-R, *Ionospheric propagation data and prediction metods required for the design of satellite services and systems*, Geneva, 2019.

[2] NASA JPL Science, "OASIS", Available at: https://science.jpl.nasa.gov/projects/oasis/, last visited January 14th, 2022.

[3] J. D. Oetting and T. Jen, "The Mobile User Objective System," Johns Hopkins APL Technical Digest, vol. 30, no. 2, pp. 103-112, 2011.

[4] R. M. Jones and J. J. Stephenson, *A versatile three-dimensional ray tracing computer program for radio waves in the ionosphere*, U.S. Department of Commerce, Washington, D.C., 1975.

[5] IRI, "International Reference Ionosphere," Available at: https://ccmc.gsfc.nasa.gov/modelweb/models/iri2016_vitmo.php, last visited January 14th, 2022.

[6] IGRF, "International Geomagnetic Reference Field," Available at: https://ccmc.gsfc.nasa.gov/modelweb/models/igrf_vitmo.php, last visited January 14th, 2022.

[7] NRLMSISE-00, "NRLMSISE-00 Atmosphere Model," Available at: https://ccmc.gsfc.nasa.gov/modelweb/models/nrlmsise00.php, last visited January 14th, 2022.

[8] E. Blanch, D. Altadill, J. M. Juan, A. Camps, J. Barbosa, G. González-Casado, J. Riba, J. Sanz, G. Vazquez, R. Orús-Pérez, "Improved characterization and modeling of equatorial plasma depletions," J. Space Weather Space Clim. 8 A38, EDP Science, 2018.

[9] SpaceWeatherLive, "Ciclos solares históricos," Available at: https://www.spaceweatherlive.com/es/actividad-solar/ciclo-solar/ciclos-solares-historicos.html, last visited January 9th, 2022.

[10] M. Nicolet, "The collision frequency of electrons in the ionosphere," *Atmospheric and Terrestrial Physics*, Pergamon Press Ltd., London, pp. 200-211, 1953.